Digest Journal of Nanomaterials and Biostructures Vol. 5, No 2, May 2010, p. 557-566

BIOREACTIVITY EVALUATION IN SIMULATED BODY FLUID OF MAGNETRON SPUTTERED GLASS AND GLASS-CERAMIC COATINGS: A FTIR SPECTROSCOPY STUDY

G. E. STAN*, A. C. POPA[a, b], D. BOJIN[c]
National Institute of Materials Physics, P.O. Box MG-7, Bucharest-Magurele, 76900, Romania
[a]*Army Center for Medical Research, CA Rosetti 37, 020012 Bucharest, Romania*
[b]*Department of Cellular and Molecular Medicine, Carol Davila University of Medicine and Pharmacy, Bucharest, Romania*
[c]*Faculty of Materials Science and Engineering, Politehnica University of Bucharest, Romania*

In this study, Fourier Transform Infrared Spectroscopy (FTIR) in Attenuated Total Reflectance mode was employed as main characterization technique to investigate the reaction mechanisms in vitro (SBF) of bioglass and glass-ceramic sputtered coatings. Two bioglass compositional systems are compared in order to gain more information regarding their in vitro bioreactivity. Important correlations between the concentration of non-bridging silicon–oxygen (Si–O–NBO) groups and the content of network modifiers were found. FTIR revealed that the high concentrations of Si–O–NBO groups are promoting the enhancing of coatings' reactivity. This information could be very useful for the development and tailoring of new bioactive glasses with an optimum biological behaviour. By varying the compositional features and the structural state, the sputtered glassy coatings exhibited different in vitro behaviour: inertness, resorbability and bioactivity.

(Received March 28, 2010; accepted May 21, 2010)

Keywords: Bioglass and Glass-ceramic films, Magnetron sputtering, SBF in vitro tests, FTIR analysis

1. Introduction

In the early 1970s, Larry Hench discovered that certain compositions of glasses in the SiO_2-CaO-Na_2O-P_2O_5 compositional system feature a bioactive behaviour – the bioglasses (BGs) [1,2]. A bioactive material elicits a specific biological response at the implant-tissue interface which results in the formation of a bond between the tissues and the implanted material. When a bioactive glass is put in contact with biological fluids, a layer of carbonated hydroxyapatite (CHA), analogue to the human bone mineral phase, forms on its surface. After these physical-chemical reactions occurred, biological moieties began to interact with newly formed apatitic layer, collagen molecules are incorporated in the CHA layer. Further after the osteogenic cells attach to collagen fibres by focal adhesion junctions they begin to divide and to synthesize the future bone matrix which will heal the lesion and integrate the implant.

BGs are considered to be osteoproductive or bioactive materials Class A [3]. Since their discovery these materials were considered for many applications in orthopaedic and dental field. However, due to their poor mechanical properties, these glasses cannot be used in load-bearing applications. During the last two decades the BGs were studied extensively in bulk form (granules, powders) such as drug delivery systems, non-load-bearing implants, and bone cements [4,5]. Due to their excellent mechanical properties metallic alloys are still the materials of choice in implantology. However, the metallic implants lack the ability of bonding directly with human

*Corresponding author: george_stan@infim.ro

bone, and need to be coated with bioactive films. Such coatings should fulfil two purposes: increasing the osseointegration of the implants, and barrier function by protecting the metal against corrosion from the body fluids and the tissue from the corrosion products of the metallic implant.

Various techniques, including enamelling [6], plasma spraying [7], sol–gel [8], electrophoretic deposition [9], and pulsed laser deposition [10,11] have been proposed to prepare high quality bioactive glass coatings. Unfortunately, many of the attempts to coat metallic implants with BGs had limited success due to the poor BG coatings adherence [6,7]. An ideal biomaterial requires both good biological and biomechanical compatibility. Radio-frequency magnetron sputtering (RF-MS) has emerged as a powerful technique for the synthesis of BG coatings due to advantages such as: extremely high adhesion of films, high-purity of the films, excellent uniformity on large area substrates, low pressure operation, low substrate temperature and ease of automation [12,13]. The amorphous BGs with low strength, are generally restricted to clinical non-load bearing cases. On the other hand the glass–ceramics, derived from bioglasses by devitrification heat-treatments, could offer a better mechanical and biological performance [14,15]. Devitrification of the bioglass in these compositional systems could lead to an increase in the elastic moduli up to ~ 30% (when fully crystallized) along with a negligible change in density [16]. Recently, we have successfully prepared adherent bioglass and glass-ceramic coatings by RF-MS [17,18].

The aim of this study was to synthesize BG thin films on Ti substrates by RF-MS and to study their bioreactivity in simulated body fluid (SBF). We focused our investigations on: (i) synthesis of bioactive glasses of the SiO_2–Na_2O–CaO–P_2O_5 compositional system with different SiO_2 contents, (ii) structural evaluation of the sputtered BG films prior and after annealing treatment in air; (iii) study of the composition influence on the BGs films stability and reactivity in vitro.

2. Experimental

2.1 *Materials*

Two bioglass powders with micrometric granular size were used as cathode targets: BG1 (45S5 Bioglass®) and BG2 (55S2). Their composition is presented in Table 1. The magnetron cathode targets (110 mm diameter, 3 mm thick) were obtained by mild pressing of the BG powders at room temperature in titanium carriers.

Medical grade Ti6Al4V plates of 10×10 mm were used as deposition substrates. In a first step the substrates were ultrasonically cleaned for 15 minutes in acetone and ethanol and then dried in nitrogen flow. Prior to deposition, the substrates were etched for 10 min at a 0.4 kV DC bias voltage in argon plasma produced by a wolfram plasmatron. This surface treatment is designed for eliminating any remaining impurities and to improve films' adhesion [17].

Table 1. Composition (in wt %) for the bioglass target powders.

Oxide	SiO_2	CaO	P_2O_5	Na_2O	K_2O	MgO
BG1 (45S5)	45	24.5	6	24.5	-	-
BG2 (55S2	55	15	10	5	10	5

2.2 Deposition procedure

The BG films were prepared using an UVN-75R1 sputtering deposition system having a magnetron planar cathode with a plasma ring of ~55 mm diameter, operating at radio-frequency of 1.78 MHz. The sputtering chamber was first evacuated to a pressure lower than 3×10^{-3} Pa. Then spectral argon was admitted through needle valves at a constant flow rate of 45 sccm. During the sputtering process the pressure was measured by a capacitive gauge (Alcatel ASD 1004).

A 0.3 Pa sputtering pressure was used for all depositions (Table 2). The sputtering of BG/Ti coatings was carried out for 1 h, at a constant and low RF power (DC_{bias} target value of 44V) in order to avoid the overheating of the target surface. A target-to-substrate distance of 30 mm was used. The substrates were not heated during deposition and their temperature (around

150°C) was only dependent on plasma self-heating. The crystallization of the chosen bioglasses starts within the 610 - 750°C range and the larger the temperature, the higher crystallization degree [19]. We have chosen for our study an annealing treatment at 700°C/2h in order to induce the partial crystallization of the coatings. Low heating and cooling rates (1°C/min) have been applied in order to minimize the residual mechanical stress in films at the end of the thermal cycle [20].

Table 2. Deposition conditions for the MS-BG sample batches.

Sample Batch	Working atmosphere	Pressure (Pa)	Gas Flow (sccm)	DC_{bias} (V)	Deposition time (min)	Thickness (nm)
BG1	Ar 100%	0.3	40	44	60	700
BG2	Ar 100 %	0.3	40	44	60	750

2.3 In vitro tests in simulated body fluid

The in vitro bioreactivity of the bioglass samples was investigated by immersion in SBF solutions with the following ionic concentrations (in mMol): 142.0 Na^+, 5.0 K^+, 2.5 Ca^{2+}, 1.5 Mg^{2+}, 147.8 Cl^-, 4.2 HCO_3^-, 1.0 HPO_4^{2-} and 0.5 SO_4^{2-}. The solutions are buffered at $pH = 7.25$ with tris-hydroxymethyl-amminomethane (Tris, 50 mM) and hydrochloric acid solutions according to Kokubo [21]. The SBF was filtered through sterilized Millipore PVDF type filters with 0.22 μm pore size. Sterilized glass flasks were used for the experiments. The volume of SBF used per sample was 10 ml and the SBF solution was not renewed during the experiment. Three replicates per sample were performed. Sampling took place at 1, 3, 7, 15, 21 and 30 days. After soaking, the samples were removed from the solution, rinsed gently, first with pure ethanol and then using deionized water, and dried at room temperature in a desiccator for 3 h. The in-vitro evolution and the chemical growth kinetics were monitored by FTIR spectroscopy measurements.

2.4 Compositional and structural characterizations

The identification of crystalline phases induced by post-deposition annealing treatments was made by grazing incidence X-ray diffraction (GIXRD) using a *Bruker D8 Advance* diffractometer, in parallel beam setting, with monochromatised Cu $K_{\alpha 1}$ radiation (λ=1.5406 Å). The incidence angle was set at 2º, and the scattered intensity was scanned in the range 5-65º (2θ), with a step size of 0.04º, and 30 seconds per step. A semi-quantitative chemical composition analysis of the as-deposited BG samples was performed by energy dispersive microanalysis (EDS) using an *Edwin WinTools* instrument. The EDS spectra were recorded at an acceleration voltage of 10 keV and mediated on a surface area of 2x2 μm^2, using a collecting time of 300 seconds per measurement. No conductive coating was applied. Fourier transform infrared spectroscopy (FTIR) was carried out using a *Perkin Elmer BX Spectrum-Pike* spectrometer in Attenuated Total Reflectance (ATR) mode for the detection of the functional groups present in the glass films before and after SBF in vitro testing. The analysis was performed within the 400 - 4000 cm^{-1} range, with a 4 cm^{-1} resolution, and a total of 50 scans per experiment.

3. Results

3.1 EDS analysis

The EDS results revealed that the targets composition was transferred quasi-stoichiometrically to the substrates. In case of both BG coatings one can notice a nearly-stoichiometric transfer for Si and Ca atoms, while the concentration strongly increase for Na, and decreases for K and Mg. The P concentration strongly decreases in case of BG1 coatings, and

increases for BG2 coatings (Table 3). One can expect that the modification of the films' composition with respect to the starting powders influences the thermal expansion coefficient of the films as well as their bioreactivity.

Table 3. Chemical compositions in at % for the BG target powder and for the BG films deposited onto titanium substrates. The values were determined by EDS for the films, and were calculated on the basis of the nominal oxides composition for the target.

Element	Si	Ca	P	Na	K	Mg
BG1 (45S5)	36.34	21.2	4.1	38.36	-	-
BG1 film	35	20	2	43	-	-
BG2 (55S2)	50.28	14.68	7.73	8.85	11.65	6.81
BG2 film	50	16	10	19	2.4	2.6

3.2 GIXRD characterizations

Figure 1-a,b displays in comparison the XRD patterns of the as-deposited and annealed BG films. The structure of the as-deposited BG1 and BG2 films is amorphous up to the experimental sensitivity limit. A strong signal originating from the Ti substrate (ICDD: 44-1294) was noticed. After heat treatment at 700°C/2h, the amorphous content decreases and newly crystalline phases are emerging.

In case of BG1 film the major crystalline phases have been identified as combeite - $Na_4Ca_4Si_6O_{18}$ (ICDD: 75-1687), wollastonite - $CaSiO_3$ (ICDD: 42-550), and Na_3PO_4 (ICDD: 76-202). In case of BG2 we have assigned the diffraction lines which appeared to $Na_2Mg(PO_3)_4$ phase (ICDD: 22-477) [17, 22].

The XRD measurements also showed that titanium is covered with a well-crystallised titanium dioxide - rutile and/or anatase after the heat-treatment at 700°C in air. Besides these the presence of titanium suboxides is also assumed which is consistent with the modification of the Ti line positions and profiles compared to that of the untreated sample. One can observe the shift of the Ti lines towards lower angles, associated with a strong broadening. Because this shift and broadening affects much more the Ti lines associated with crystalline planes whose spacing is related to the *c* axis period, we are tempted to explain it by the diffusion of oxygen between the planes with hexagonal symmetry of the Ti lattice.

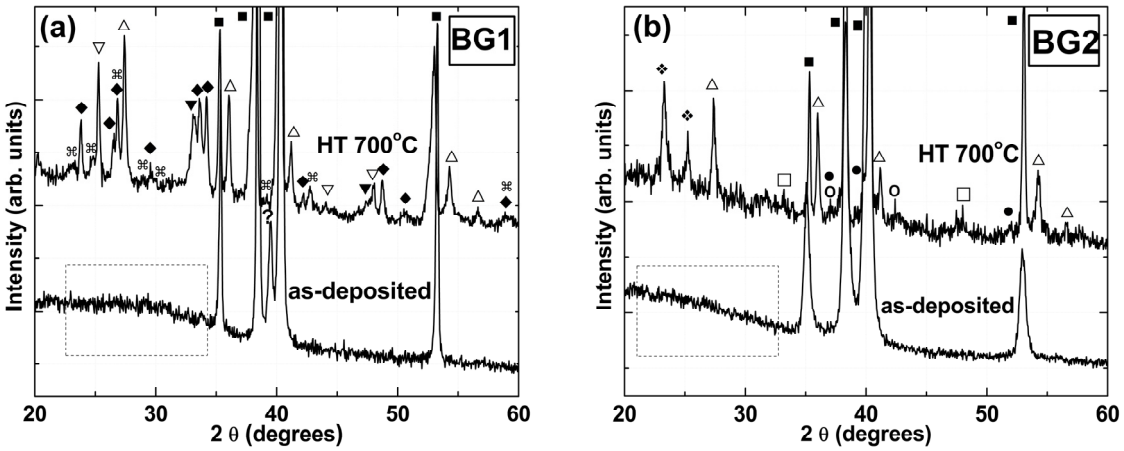

Fig. 1. XRD diagrams of BG films before and after heat treatment at 700°C/2h in air. (a) BG1: ◆=$Na_4Ca_4Si_6O_{18}$ (combeite); ▼=Na_3PO_4; ⌘=$CaSiO_3$ (wollastonite); △= TiO_2-rutile, ▽=TiO_2-anatase; ?=possible titanium sub-oxides, and ■= Ti; (b) BG2: ❖ = $Na_2Mg(PO_3)_4$, △ = TiO_2-rutile, O = $CaTiO_3$, ● = Ti_2O, □ = TiO, and ■= Ti.

3.3 FTIR studies

The bioglass structure is very complex, there is no long range order, but it exhibits some short and medium range order. The silica-based glass structure is generally viewed as a matrix composed of SiO_4 tetrahedra connected at the corners to form a continuous tri-dimensional network with all bridging oxygen (BOs). The SiO_4 tetrahedra network is slightly distorted due to variations in the bond angles and the torsion angles. The network modifiers (alkali and alkali-earth ions typical to bioglasses) enter the structure as singly or double charged cations and occupy interstitial sites. Their charge is compensated by non-bridging oxygen bonds (NBOs), created by breaking bridges between adjacent SiO_4 tetrahedra. The increase of modifier content generates the creation of large NBOs concentrations, reducing the connectivity of the BG network, with direct effect upon electrical conduction, the thermal expansion coefficient, glass transition temperature, chemical corrosion in aqueous media and bioactivity [23,24].

FTIR spectroscopy is a powerful method to obtain useful information concerning the short-range order for the as-deposited amorphous films as well as for SBF tested films, allowing the identification of specific features in the IR vibrational spectrum, such as those related to silicate or phosphate groups.

Figure 2-a,b shows the FTIR spectra of the as-deposited and heat-treated BG films together with the spectrum of target powder. The infrared absorption spectra, recorded in ATR technique, show a very similar absorption envelope for the target and as-deposited BG films, exhibiting the same broad IR bands typical to an amorphous structure. Moreover for the as-deposited BG films it presents a shift to higher wave numbers of the maximum absorption peak.

The IR spectra (*Figure 2-a*) of BG1 structures revealed three strong vibration bands:

- 924 - 944 cm^{-1} - attributed to the stretching vibration of the SiO_4 units with three and two non-bridging oxygen atoms, the Q^1 (Si-O-3NBO), and Q^2 (Si-O-2NBO) groups;
- 1010-1022 cm^{-1} assigned to the coexistence of various Q^2 and Q^3 Si-O-Si asymmetric stretching vibration;
- 766 cm^{-1} corresponding to the bending motion of the oxygen atom Si-O(b) along the bisector of the Si–O–Si bridging group [25, 26].

The weaker band at 680 cm^{-1} might correspond to symmetric stretching bands of PØP Q3 in Q^2 and Q^1 units. Other vibrations of phosphate groups present in the bioglass are difficult to emphasize because of the superimposition of the strong bands of SiO_4 units. Previous IR studies noticed also the presence of Q^2, Q^1, and Q^0 phosphate units in the 1400–400 cm^{-1} IR spectra range [25, 26]. The weak broad shoulder present at 1600 cm^{-1} can be assigned to water bending vibrations, indicating that BG1 material is highly hygroscopic, absorbing water vapour when in air. The presence of absorption band at 1439 cm^{-1} is attributed to the stretching vibrations of carbonate $(CO_3)^{2-}$ structures incorporated during the deposition process. After the post-deposition annealing a clear splitting of the bands was noticed, pointing a strong crystallization of the BG coating, in agreement with the GIXRD measurements.

In case of BG2 structures (*Figure 2-b*) we noted the presence of three intense vibration bands:

- 1001-1030 cm^{-1} assigned to asymmetric stretching vibrations of Si-O-Si in the Q^2 and Q^3 units;
- 1102-1130 cm^{-1}, more intense for the as-deposited samples could be attributed to the anti-symmetric stretching mode of Si–O–Si groups.
- 794 cm^{-1} corresponding to the bending motion of the oxygen atom Si-O(b) along the bisector of the Si–O–Si bridging group [25,26].

The peak at 1383 cm^{-1} might be assigned to a shifted $(CO_3)^{2-}$ stretching band. The presence of the weaker band at 696 cm^{-1} corresponds to symmetric stretching bands of PØP Q^3 in Q^2 and Q^1 units. After the heat-treatment at 700°C/2h one can observe the splitting of the envelope in two shoulders, indicating a crystallization of the BG structure, along with the appearance of new vibration band at 910 cm^{-1} (the stretching of the Si-O-3NBO and Si-O-2NBO) groups). A strong shift to lower wave numbers of the bands positioned at 1030 and 1120 cm^{-1} was also noticed.

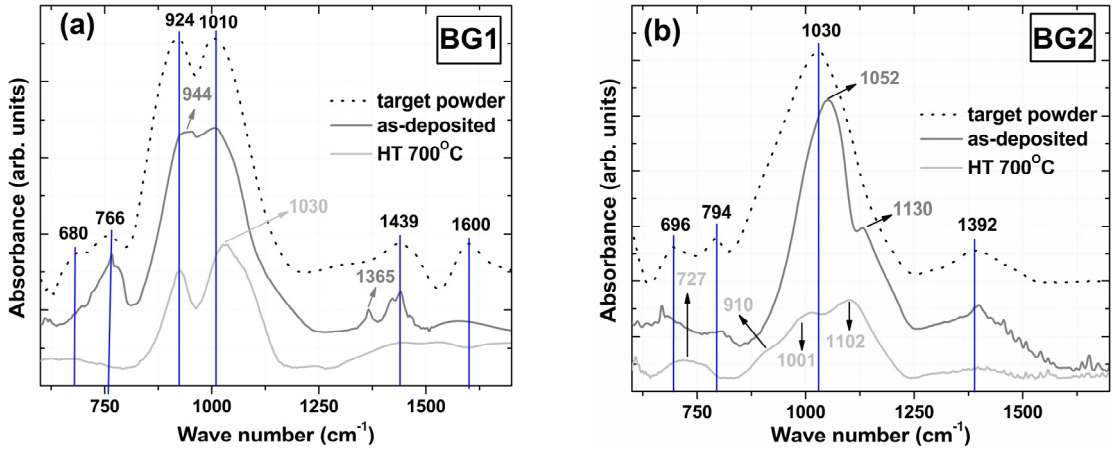

Fig. 2. Comparative FTIR spectra for the target powders and the studied films: a) BG1; b) BG2.

Figure 3 displays a comparison of the BG films IR spectra before and after immersion in simulated body fluid up to 30 days.

In case of as-deposited BG1 samples (*Figure 3-a*) after only 24 hours of immersion, dramatic changes were observed. The spectrum revealed the disappearance of the initial BG film vibration bands and the emergence of two new and strong bands positioned at 816 and 1107 cm^{-1}, which could be assigned to bending and stretching bands of the amorphous silica phase [27]. Weaker bands at 736, 892 and 968 cm^{-1}, were noticed, belonging most probably to the original BG layer. The intensity of these bands decreased with the immersion time suggesting a continuously leaching of BG ions into the SBF solution. After 30 days of immersion the BG films is completely dissolved, no IR bands could be emphasized, indicating the resorbability of this material.

The FTIR results of the annealed BG1 samples after in-vitro testing in SBF are presented in *Figure 3-b*. After 24 hours soaking in SBF solution the amplitude of the peak at 924 cm^{-1} present increased values and displaced at ~ 940 cm^{-1}. This maximum peak at 940 cm^{-1} is also present related to the Si-OH groups [11,20]. In comparison the peak positioned at 1030 cm^{-1} is decreased in amplitude. The process could be related to the continuous leaching of Na, Ca and Si ions in the SBF solution. The exchange of the ions between the surface layer and SBF solution lead to a rearranging of the bonds in the sample surfaces. At the same time the diffusion of the H^+ ions, because of the increase of the electronegativity of the surface toward the BG films will initiate the formation of the Si-OH bonds on their surface [1,20]. The small shoulder at 895 cm^{-1} revealed the presence of the stretching vibrations of the Si-O bonds with two non-bridging oxygens (Q^1 and Q^0 units) from the original BG layer. After 72 hours of immersion in SBF solution the peaks at 776 and 1030 cm^{-1} increased in amplitude suggesting the enrichment of the Si-O-Si bonds in the SiO_4 tetrahedra (Q^4 units). This suggests that after a certain period of time the polymerization reaction begins at the film surface. Also, the peak at 940 cm^{-1} strongly decreases in amplitude, revealing three new weak bands at 960 cm^{-1}, 1021 and 1087 cm^{-1} respectively. These absorption bands are assigned to ν_1 symmetric stretching mode of $(PO_4)^{3-}$ (960 cm^{-1}) and to ν_3 asymmetric stretching of the phosphate groups, respectively (1021 and 1087 cm^{-1} bands) [28].

This phenomena could be related to simultaneous phenomena such: formation of the silicic acid $Si(OH)_4$ and subsequent polycondensation reaction, along with the beginning of the precipitation of calcium phosphate (Ca-P) phases on the surface from the SBF solution suprasaturated in Ca-P ions [20]. The released water in the polycondensation reaction is known to remain physically bonded with the Si-O-Si surface forming the hydrated silica rich layer [1,2]. This is leading to an increase of the pH at the surface level which will be favourable to the absorption of the cations and anions on the surface, the precipitation processes of Ca-P rich phases being under these auspicious conditions.

The process of precipitation seems to continue up to 30 days, the relative integral area of the bands at 960 cm^{-1}, 1021 and 1087 cm^{-1} monotonously increasing with immersion time. Thus, it is suggested that on top of the annealed BG1 coatings chemically develops in vitro a Ca-P type layer. The broad aspect of the bands suggests the amorphous nature of this chemically grown

layer. For comparison the spectrum of a crystalline synthetic hydroxyapatite powder is displayed. No crystallization processes were observed in XRD after 30 days of immersion.

For the as-deposited and annealed BG2 structures, the FTIR measurements (*Figure 3-c,d*) showed no changes in intensity and position of the original vibration bands with immersion time, suggesting the inert character of this material.

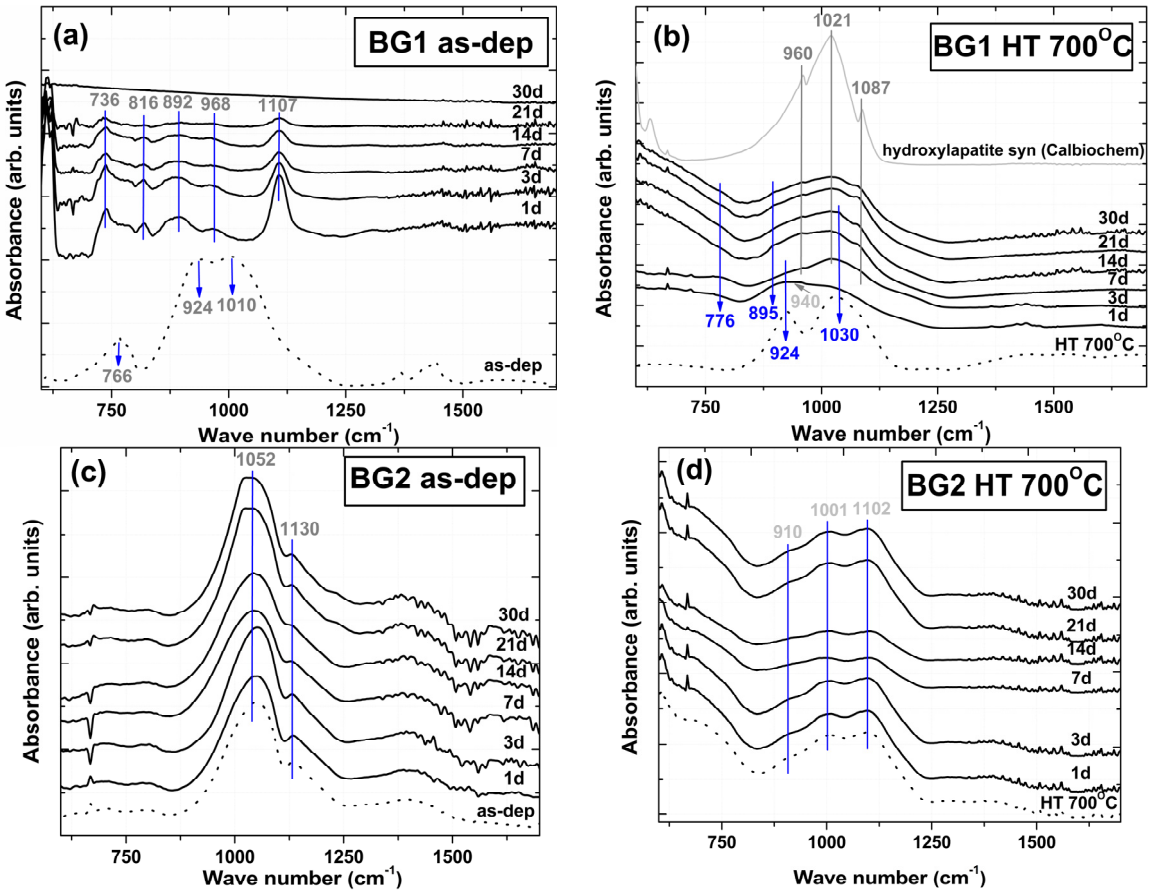

Fig. 3. Evolution of FTIR spectra of the BG films with increasing immersion time in SBF (1 - 30 days).

4. Discussion

The bioactivity of a bioglass or glass-ceramic is primarily influenced by the concentrations of bridging and non-bridging oxygen atoms per silicon oxygen tetrahedron as a function of the alkali and alkali earth oxide content [23,24]. The shifts towards higher wave numbers of several distinct bands of the BG films in comparison with the powder spectrum could be explained by the mechanical stresses present in thin films in comparison with the powder state. However, these shifts might also indicate a certain degree of modification of the silicate tetrahedron network during sputtering, which can be correlated with the composition modification.

The mechanism of calcium phosphates formation onto the surface of bioactive glasses is widely accepted, and involves the dissolution of cations from the surface of bioactive glasses and the consequent increase of the supersaturation degree in the surrounding fluid, with respect to HA components. Hench's theory states that the first stage of a bioglass mineralization upon immersion in SBF involves the rapid exchange of Na^+ ions from the glass for H^+ and H_3O^+ ions from the solution, which shall initialize the breaking of the Si-O-Si bonds of the glass structure and the subsequent formation of silanol groups. In a next step the silanol groups polycondensate forming a silica-rich layer at the bioglass surface, which favours the growth of Ca-P type layers [1,29].

The IR spectra of the samples immersed in SBF for 1 month showed different behaviour in vitro function of composition and crystallization state. In case of as-deposited BG1 samples a continuous dissolution process occurs, after 30 days the entire film is dissolved into the surrounding fluid. One can notice the high content of Ca (~ 20 at.%) and Na atoms (~ 43 at.%) in the BG1 film (*Table 3*). It can be speculated that when very high numbers of alkali and alkali-earth ions are released in SBF, the pH will rapidly and drastically change at the film-fluid interface, producing a chemical unbalance which will suppress the polymerization of silanols and the further formation of the SiO_2-rich surface layer. The bioactive process is thus disrupted, leading to continuous dissolution of the BG amorphous film. On the other hand the annealing of BG1 films followed by slow cooling promotes formation of combeite, wollastonite and Na_3PO_4, which have smaller solubility, and consequently a decreased leaching rate of Na^+ and Ca^{2+} into the SBF solution. This will determine the conditions at the surface of the film to be more stable, therefore allowing polymerisation of soluble $Si(OH)_4$ in a SiO_2-rich layer which will act as a nucleation site for apatite [1]. During 30 days of SBF soaking, dissolution-reprecipitation processes took place, the annealed BG1 layer is partially dissolved and finally we obtain a multilayer structure containing a bottom BG layer coated by an amorphous SiO_2-rich thin film and at the top a Ca-P type layer. Thus in case of BG1 annealed samples our FTIR results are consistent with Hench's theory. Previous studies have also reported that both the combeite [30] and wollastonite [31] can generate on their surface Ca/P rich layers when in contact with SBF. The growth of the bioapatite layer is essential for bone generation and bonding ability. However, the combeite was proved to rapidly transform into amorphous calcium phosphate phase in contact with SBF, but it delays the process of crystallization into a hydroxyapatite phase [1]. Besides biocompatibility, these structures could actively improve proteins and osteocytes adhesion, significantly shortening the osteointegration time. The inertness of BG2 structures might be determined by their chemical composition. High contents of SiO_2 have influences both in bioactivity and the thermal expansion coefficient of the glass. In general, SiO2-rich glasses with silica contents higher than 60 wt.% have a better mechanical stability and adhesion to the metallic substrate, but are not soluble in body fluids [32,33]. Decreasing the silica content is therefore mandatory for improving the bioactivity and partial dissolution of the glass surface. For the BG2 structures one can notice an important silicon (~ 50 at.%) and phosphorous content (~ 10 at.%). In silica-based glasses phosphorous acts as a network former producing structural rearrangement where the silicate network is more interconnected by creating P-O-Si cross-links. At higher content of phosphorus, the glass is increasing in connectivity. The glass compositions with higher content of network formers, do not bond either to bone or to soft tissues and elicit formation of a non-adherent fibrous interfacial capsule [34,35]. No surface changes during SBF tests were evidenced for the annealed BG2 structure. Unlike in case of BG1, the crystallization had no effect on BG2's surface reactivity. The nucleated $Na_2Mg(PO_3)_4$ phase proved to be inert in SBF. It can be concluded that the chemical composition, bonding configuration and crystallinity could play important roles in BG films' reactivity in SBF. For achieving bioactive properties an optimal ratio of network formers/network modifiers is required, but not sufficient. The disruption of the Si-O-Si bonds and creation of Si-O-NBO bonds, determined by increased network modifiers content, is mandatory in the first steps of Ca-P chemical growth mechanism. Although BG compositions with very high network modifier content have a native poor stability, we can tailor their in-vitro behaviour by thermal treatments of crystallization to obtain the best bioactive outcome.

5. Conclusions

The study evaluated the influence of chemical composition, bonding state, and post-deposition annealing treatment upon the sputtered BG films' bioreactivity in simulated body fluid. The best results of bioactivity were obtained for the 45S5 layers annealed at 700°/2h in air. The high concentration of Si–O–NBO groups and devitrification favours an appropriate biological response in simulated body fluid. These magnetron sputtered glass-ceramic films are promising for further research in vitro tests in osteogenic cells cultures.

Acknowledgements

Authors are grateful to Ionut Enculescu and Iuliana Pasuk for the professional assistance with EDS characterizations and GIXRD measurements. The financial support of "BD" PhD research scholarship offered by CNCSIS is gratefully acknowledged by G.E. Stan.

References

[1] L. L. Hench, J. Wilson, An Introduction to Bioceramics, 1st ed., World Scientific Publishing Company, Singapore (1993).
[2] L. L. Hench, J. Am. Ceram .Soc. **74**, 1487 (1991).
[3] J. Wilson, S. J. Low, J. Appl. Biomat. **3**, 123 (1992).
[4] Z. P. Xie, C. Q. Zhang, C. Q. Yi, J. J. Qiu, J. Q. Wang, J. Zhou, J. Biomed. Mater. Res. B Appl. Biomater. **90**, 195 (2009).
[5] M. Vogel, C. Voigt, U.M. Gross, C.M. Müller-Mai, Biomaterials **22**, 357 (2001).
[6] L. Peddi, R. K. Brow, R.F. Brown, J. Mater. Sci-Mater. Med. **19**, 3145 (2008).
[7] G. Goller, Ceram. Int. **30**, 351 (2004).
[8] I. Izquierdo-Barba, F. Conde, N. Olmo, M. A. Lizarbe, M. A. Garcia, M. Vallet-Regi, Acta Biomater. **2**, 445 (2006).
[9] A. Balamurugan, G. Balossier, J. Michel, J. M. F. Ferreira, Electrochim. Acta **54**, 1192 (2009).
[10] A. C. Popescu, F. Sima, L. Duta, C. Popescu, I. N. Mihailescu, D. Capitanu, R. Mustata, L. E. Sima, S. M. Petrescu, D. Janackovic, Appl. Surf. Sci. **255**, 5486 (2009).
[11] C. Berbecaru, H.V. Alexandru, A. Ianculescu, A. Popescu, G. Socol, F. Sima, I. Mihailescu, Appl. Surf. Sci. **255**, 5476 (2009).
[12] K. Wasa, M. Kitabatake, H. Adachi, Thin Film Materials Technology: Sputtering of Compound Materials, Noyes Publications, New York (2003).
[13] G.E. Stan, J. Optoelectron. Adv. Mater. **11**, 1132 (2009).
[14] W. Bonfield, M. Wang, K. E. Tanner, Acta Mater. **46**, 2509 (1998).
[15] O. Peitl Filho, G.P. LaTorre, L.L. Hench, J. Biomed. Mater. Res. **30**, 509 (1996).
[16] C.C. Lin, L.C. Huang, P.Y. Shen, J. Non-Cryst. Solids **351**, 3195 (2005).
[17] G. E. Stan, C. O. Morosanu, D. A. Marcov, I. Pasuk, F. Miculescu, G. Reumont, Appl. Surf. Sci. **255**, 9132 (2009).
[18] G. E. Stan, S. Pina, D. U. Tulyaganov, J. M. F. Ferreira, I. Pasuk, C. O. Morosanu, J. Mater. Sci.-Mater. Med. **21**, 1047 (2010).
[19] L. Lefebvre, J. Chevalier, L. Gremillard, R. Zenati, G. Pollet, D. Bernache-Assolant, A. Govin, Acta Mater. **55**, 3305 (2007).
[20] C. Berbecaru, H. V. Alexandru, G. E. Stan, D. A. Marcov, I. Pasuk, A. Ianculescu, Mater. Sci. Eng. B **169**, 101 (2010).
[21] T. Kokubo, H. Kushitani, C. Ohtsuki, S. Sakka, T. Yamamuro, J. Mater. Sci.-Mater. Med. **4**, 1 (1993).
[22] B. Thonnerieux, J. C. Grenier, A. Durif, C. Martin, CR Seances Acad. Sci. C **267**, 968 (1968).
[23] J. Serra, P. González, S. Liste, S. Chiussi, B. León, M. Pérez-Amor, H. O. Ylänen, M. Hupa, J. Mater. Sci.-Mater. Med. **13**, 1221 (2002).
[24] S. Liste, J. Serra, P. González, J. P. Borrajo, S. Chiussi, B. León, M. Pérez-Amor, Thin Solid Films **453 –454**, 224 (2004).
[25] G. Socrates, Infrared and Raman Characteristic Group Frequencies—Tables and Charts, John Wiley & Sons Ltd. (2007).
[26] S. Agathopoulos, D. U. Tulyaganov, J. M. G. Ventura, S. Kannan, M. A. Karakassides, J. M. F. Ferreira, Biomaterials **27**, 1832 (2006).
[27] R. Bal, B.B. Tope, T.K. Das, S.G. Hegde, S. Sivasanker, J. Catal. **204**, 358 (2001).
[28] M. Markovic, B. O. Fowler, M. S. Tung, J. Res. Natl. Inst. Stand. Technol. **109**, 553 (2004).
[29] F. C. M. Driessens, R. M. H. Verbeeck, Biominerals, CRC Press Inc, Boca Raton, (1990).
[30] Q. Z. Chen, I. D. Thompson, A. R. Boccaccini, Biomaterials **27**, 2414 (2006).

[31] W. Xue, X. Liu, X. Zheng, C. Ding, Biomaterials **26**, 3455 (2005).
[32] D. Tanaskovic, B. Jokic, G. Socol, A. Popescu, I.N. Mihailescu, R. Petrovic, Dj. Janackovic, Appl. Surf. Sci. **254**, 1279 (2007).
[33] S. Lopez-Esteban, E. Saiz, S. Fujino, T. Oku, K. Suganuma, A. P. Tomsia, J. Eur. Ceram. Soc. **23**, 2921 (2003).
[34] A. Tilocca, A. N. Cormack, J. Phys. Chem. B **111**, 14256 (2007).
[35] A. Tilocca, Proc. R. Soc. A **465**, 1003 (2009).